PNAS RESEARCH ARTICLE | MICROBIOLOGY

Hepatitis E virus infects brain microvascular endothelial cells, crosses the blood–brain barrier, and invades the central nervous system

Debin Tian[a], Wen Li[a], C. Lynn Heffron[a], Bo Wang[a], Hassan M. Mahsoub[a], Harini Sooryanarain[a,b], Anna M. Hassebroek[a], Sherrie Clark-Deener[c], Tanya LeRoith[a,b], and Xiang-Jin Meng[a,b,1]

Contributed by Xiang-Jin Meng; received February 1, 2022; accepted May 4, 2022; reviewed by Alexander Ploss and Christopher Walker

Hepatitis E virus (HEV) is an important but understudied zoonotic virus causing both acute and chronic viral hepatitis. A proportion of HEV-infected individuals also developed neurological diseases such as Guillain–Barré syndrome, neuralgic amyotrophy, encephalitis, and myelitis, although the mechanism remains unknown. In this study, by using an in vitro blood–brain barrier (BBB) model, we first investigated whether HEV can cross the BBB and whether the quasi-enveloped HEV virions are more permissible to the BBB than the nonenveloped virions. We found that both quasi-enveloped and nonenveloped HEVs can similarly cross the BBB and that addition of proinflammatory cytokine tumor necrosis factor alpha (TNF-α) has no significant effect on the ability of HEV to cross the BBB in vitro. To explore the possible mechanism of HEV entry across the BBB, we tested the susceptibility of human brain microvascular endothelial cells lining the BBB to HEV infection and showed that brain microvascular endothelial cells support productive HEV infection. To further confirm the in vitro observation, we conducted an experimental HEV infection study in pigs and showed that both quasi-enveloped and nonenveloped HEVs invade the central nervous system (CNS) in pigs, as HEV RNA was detected in the brain and spinal cord of infected pigs. The HEV-infected pigs with detectable viral RNA in CNS tissues had histological lesions in brain and spinal cord and significantly higher levels of proinflammatory cytokines TNF-α and interleukin 18 than the HEV-infected pigs without detectable viral RNA in CNS tissues. The findings suggest a potential mechanism of HEV-associated neuroinvasion.

hepatitis E virus (HEV) | neurological disorder | central nervous system (CNS) | blood–brain barrier (BBB) | brain microvascular endothelial cells

Significance

Hepatitis E virus (HEV) causes not only acute and chronic hepatitis but also neurological disorders. To delineate the mechanism of HEV-associated neurological diseases, we showed that both quasi-enveloped and nonenveloped HEVs can cross the blood–brain barrier model in a tumor necrosis factor alpha (TNF-α)-independent manner and productively infect brain microvascular endothelial cells in vitro. Furthermore, we showed that HEV was detected in brain and spinal cord from HEV-infected pigs and that pigs with detectable HEV in central nervous system (CNS) tissues had histological lesions in brain and spinal cord and significantly higher levels of proinflammatory cytokines TNF-α and interleukin 18 than pigs without detectable HEV in CNS tissues. The results shed light on a potential mechanism of HEV-associated neuroinvasion.

Hepatitis E virus (HEV), an important emerging human pathogen, infects humans and a plethora of other animal species (1, 2). In humans, HEV primarily causes self-limiting acute viral hepatitis worldwide. It is estimated that there are ∼20 million HEV infections annually, leading to ∼3.4 million clinical cases of hepatitis E and 70,000 hepatitis E-related deaths globally (3). In industrialized countries, clinical cases of hepatitis E are mainly sporadic or clustered in nature, while in developing countries endemic or epidemic hepatitis E is occasionally associated with large outbreaks (4, 5). The main route of HEV transmission is fecal–oral, via contaminated drinking water or consumption of undercooked animal meat products (6). Since the discovery of swine HEV in 1997 from pigs in the United States (7, 8), novel strains of HEV have now been genetically identified from more than a dozen animal species, including domestic and wild pig, rabbit, camel, rat, chick, mongoose, and deer, among others (7, 8). Some of these animal HEVs, such as swine HEV, rat HEV, deer HEV, camel HEV, and rabbit HEV, have been shown to cross species barriers and infect humans (8–10). Hepatitis E is now recognized as an important zoonotic disease with a large number of animal reservoirs, which raises further public health concerns (4, 11).

HEV-associated extrahepatic manifestations have increasingly become significant clinical problems (12), including chronic HEV infections in immunosuppressed individuals (13, 14), high mortality in HEV-infected pregnant women (15), and HEV-associated neurological and renal diseases (16–19). HEV-associated nerve root and plexus sequelae, such as Guillain–Barré syndrome and neuralgic amyotrophy, have been reported in a significant proportion of HEV-infected individuals worldwide (20, 21). Additionally, HEV-associated central nervous system (CNS) disorders, such as encephalitis, myelitis, cerebral ischemia, and seizures, have also been reported in HEV-infected patients (22–27). These neurological diseases are almost exclusively associated with zoonotic genotype 3 HEV infection, and to a lesser extent zoonotic genotype 4 HEV infection (28, 29). Although the exact mechanism how HEV infection

Author contributions: D.T., W.L., and X.-J.M. designed research; D.T., W.L., C.L.H., B.W., H.M.M., H.S., A.M.H., S.C.-D., and T.L. performed research; W.L. contributed new reagents/analytic tools; D.T., W.L., T.L., and X.-J.M. analyzed data; D.T., W.L., and X.-J.M. wrote the paper; and X.-J.M. wrote the grant and supervised the team.

Reviewers: A.P., Princeton University; and C.W., Nationwide Children's Hospital.

The authors declare no competing interest.

[1]To whom correspondence may be addressed. Email: xjmeng@vt.edu.

This article contains supporting information online at http://www.pnas.org/lookup/suppl/doi:10.1073/pnas.2201862119/-/DCSupplemental.

Published June 7, 2022.

leads to neurological diseases remains largely unknown, there is evidence suggesting that HEV may cross the blood–brain barrier (BBB) (30–33).

HEV is a single-stranded, positive-sense RNA virus in the family of *Hepeviridae*, which consists of two genera: genus *Orthohepevirus* (species A, B, C, and D) infecting mammals and avian species and genus *Piscihepevirus* infecting cutthroat trout (34). Among the eight different HEV genotypes (HEV-1 to HEV-8) in species *Orthohepevirus A* (35), HEV-3 and HEV-4 are zoonotic, infecting humans and other animal species (8, 36). The genome of HEV consists of three partially overlapping open reading frames (ORFs). ORF1 encodes nonstructural proteins (37). ORF2 encodes the antigenic capsid protein ($ORF2^c$) that induces neutralizing antibodies, as well as a secreted form of capsid ($ORF2^s$) that inhibits antibody-mediated neutralization (38). ORF3 encodes a small phosphoprotein that is a functional iron channel involved in virus replication (39). The HEV virion has two forms: The exosome-like membrane-associated quasi-enveloped virions were found in the circulating blood and in cell culture supernatant of HEV-infected cells; the nonenveloped virions were found in feces and bile of infected hosts (40–42). It is known that exosome can migrate relatively freely across the BBB (43, 44). Whether the exosome-like quasi-enveloped HEVs are more permissible to BBB entry requires investigation.

In this study, we conducted both in vitro and in vivo studies to delineate the potential mechanism of HEV-associated neuroinvasion. By using an in vitro BBB cell culture model, we first tested the ability and mechanism of membrane-associated quasi-enveloped HEV virions as well as the nonenveloped HEV virions to cross the BBB. Additionally, we also investigated the ability of both quasi-enveloped and nonenveloped HEV virions to invade CNS tissues in experimentally infected pigs. Our results suggest that HEV productively infects brain microvascular endothelial cells, crosses the in vitro BBB, and invades CNS in experimentally infected pigs.

Results

Successful Generation of Two Different Strains of Quasi-Enveloped and Nonenveloped Genotype 3 HEV (Strains P6 and US2) Virus Stocks. HEV exists as membrane-associated quasi-enveloped virions which predominantly circulate in the blood of an infected host in vivo and in the culture supernatant of infected cells in vitro and nonenveloped virions which are mainly found in feces and bile of infected host (41, 42). To produce the quasi-enveloped HEV stain P6 (eP6) virus stock, we transfected Huh7-S10-3 human liver cells with full-length capped genomic RNAs that were transcribed from the HEV P6 infectious clone. The cell culture supernatant, which contains eP6 virions, was pooled and concentrated to produce the eP6 virus stock. The viral genomic RNA copy number of the eP6 virus stock, as quantified by qRT-PCR, was ~1.0×10^8 per mL (Fig. 1*A*). The

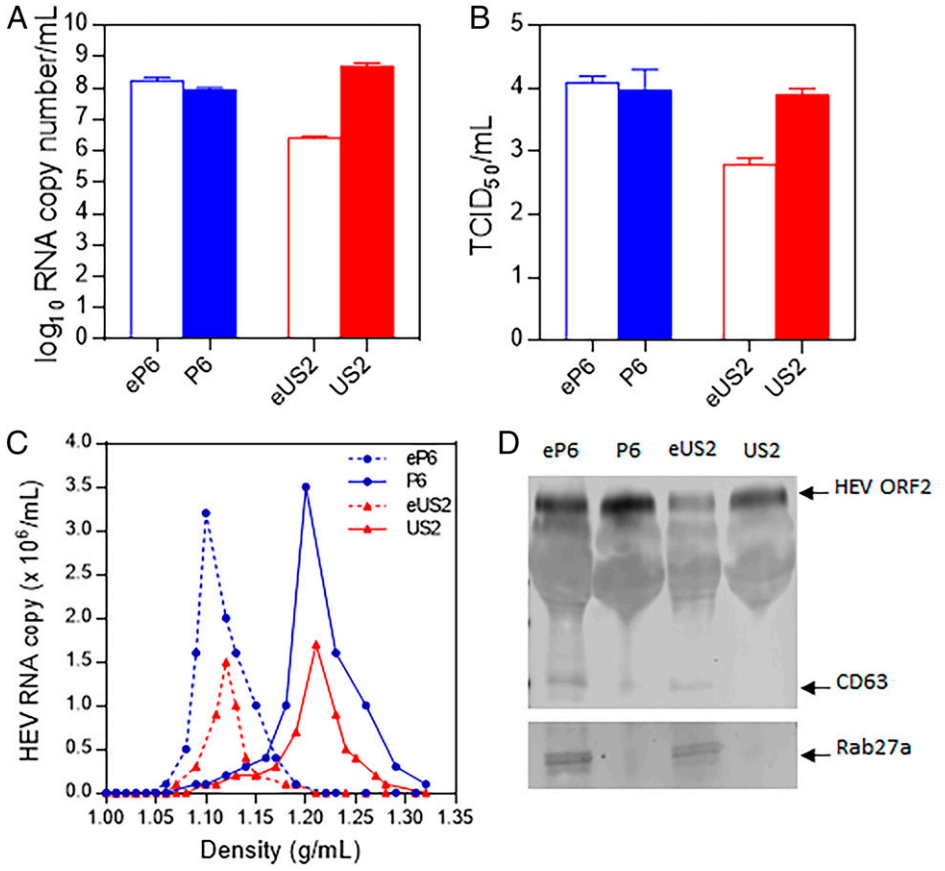

Fig. 1. Generation of membrane-associated quasi-enveloped and nonenveloped HEV virions from two different strains of genotype 3 HEV. In vitro-transcribed full-length genomic RNA from the genotype 3 HEV (strain Kernow-C1/P6) infectious clone was transfected into Huh-7 S10-3 liver cells. The culture supernatants of the transfected cells were collected and concentrated via ultracentrifugation as the virus stock of the quasi-enveloped eP6 virus. The eP6 virus was treated by detergents to produce the nonenveloped P6 virus stock. The 10% fecal suspension from a pig experimentally infected with HEV (strain US2) was purified via centrifugation and filtration to produce the nonenveloped US2 virus stock. The US2 virus was then used to infect HepG2 liver cells to generate the quasi-enveloped eUS2 virus stock. The virus stocks produced in this study were quantified by qRT-PCR to determine the genomic RNA copy numbers (*A*) and the infectious virus titer ($TCID_{50}$ per milliliter) in Huh-7 S10-3 cells (*B*). (*C*) Sucrose density gradient fractionation of the virus stocks produced in this study. (*D*) The virus stocks were analyzed via Western blot analyses using antibodies against HEV ORF2 protein and exosome markers (CD63 and Rab27a).

infectious titer of the eP6 virus stock was ~2.0 × 10^4 $TCID_{50}$ (tissue culture infectious dose) per mL as determined by infectious viral titer titration on Huh7-S10-3 cells (Fig. 1*B*). Since the quasi-enveloped HEV virions are covered with a lipid membrane, we subsequently used detergents (DOC-Na and trypsin) to remove the lipid membrane in order to produce the nonenveloped HEV virion P6. The results showed that the P6 virus stock had viral titers similar to the quasi-enveloped eP6 virus stock (Fig. 1 *A* and *B*).

As an infectious clone for HEV strain US2 is not available, we produced the quasi-enveloped US2 (eUS2) virus stock by infecting human HepG2 liver cells with the nonenveloped US2 virus stock, which was prepared previously from feces of experimentally infected pigs (45). The results showed that the generated eUS2 virus stock had a relatively lower titer (~3.0 × 10^6 genomic RNA copy number per mL, 6.0 × 10^2 $TCID_{50}$ infectious titer per mL) (Fig. 1 *A* and *B*). The nonenveloped US2 virus stock had higher titers (~5.0 × 10^8 genomic RNA copy number per mL and 1.0 × 10^4 $TCID_{50}$ infectious titer per mL).

The generated quasi-enveloped and nonenveloped virus stocks from two different strains of genotype 3 HEV were verified through density centrifugation. Sucrose density gradient data showed that there is a clear difference between the quasi-enveloped and nonenveloped virions (Fig. 1*C*): The quasi-enveloped HEV virions had a density of ~1.10 to 1.12 g/mL, while the nonenveloped HEV virions had a density of ~1.18 to 1.21 g/mL. The virus stocks were also further verified by immunoblotting analysis. The exosome markers of CD63 and Rab27a were detected in both eP6 and eUS2 viruses (Fig. 1*D*) but were absent in P6 and US2 viruses. Collectively, these data showed that we have successfully produced the quasi-enveloped HEV eP6 and eUS2, as well as the nonenveloped HEV P6 and US2.

Both Quasi-Enveloped and Nonenveloped HEV Virions Can Cross the BBB In Vitro. The brain microvascular endothelial cells (hCMEC/D3) grown in the polytetrafluoroethylene (PTFE) membrane transwell insert has been demonstrated to be a suitable in vitro culture model to mimic BBB in vivo. After 5 d of culture (2 d with hCMEC/D3 complete media and 3 d with astrocyte-conditioned media), the tight junction (TJ) formation in the barrier was confirmed via the permeability assay using FITC-dextran (4 kDa and 40 kDa), which showed that the established in vitro BBB has a significantly decreased permeability rate compared to the control, but a very small amount of FITC-dextran (<5%) still passes through the in vitro BBB (Fig. 2*A*). Also, the selected TJ marker proteins ZO-1, Gai2, occludin, and claudin-5 were expressed as stained by immunofluorescence assay (IFA) with respective marker-specific antibody.

By using the established in vitro BBB culture model, we investigated whether the quasi-enveloped and nonenveloped HEV virions can cross the barrier. As shown in Fig. 2*B*, after an input of 1.0 × 10^6 genomic RNA copies of eP6 or P6 viruses into luminal space of the BBB culture inserts, we detected the total HEV RNA copy number in the abluminal space from 8 hour postinoculation (hpi) onwards. The amount of HEV RNA in the abluminal space accumulated over time, and reached the peak titer after 48 hpi. There was no significant difference in the amount of HEV RNA between eP6 and P6 viruses at different time points. Similar results were also found for the eUS2 and US2 viruses (Fig. 2*C*). This result suggested that both quasi-enveloped and nonenveloped HEV virions are capable of crossing the BBB in vitro.

HEV Virions Cross a BBB Culture Model in a Tumor Necrosis Factor Alpha (TNF-α)-Independent Manner. It has been reported that proinflammatory cytokines such as TNF-α can promote BBB breakdown, thereby facilitating the entry of molecules into the CNS, and that TNF-α production is elevated during HEV infection (45–47). Therefore, in this study we evaluated the potential effect of TNF-α on the ability of HEV to cross the BBB in an in vitro BBB culture model. When the BBB culture model was incubated with different concentrations of the TNF-α (0 to 1,000 ng/mL) for different lengths of time (4, 8, or 16 h) prior to HEV inoculation, we found that the quasi-enveloped HEV eP6 virus readily crossed the BBB, with no significant difference among different concentrations or different lengths of incubation time (Fig. 3 *A*–*C*). Similar results were also obtained for the nonenveloped HEV P6 virus (Fig. 3 *D*–*F*). These data suggested that, under in vitro BBB culture conditions, TNF-α, which is elevated in infected individuals during HEV infection, does not appear to significantly facilitate HEV entry across the in vitro BBB.

HEV Crosses the BBB Possibly via Direct Infection of Brain Microvascular Endothelial Cells. We investigated the potential mechanism how HEV virions cross the BBB by utilizing an in vitro BBB culture model. At 48 h after inoculation of the

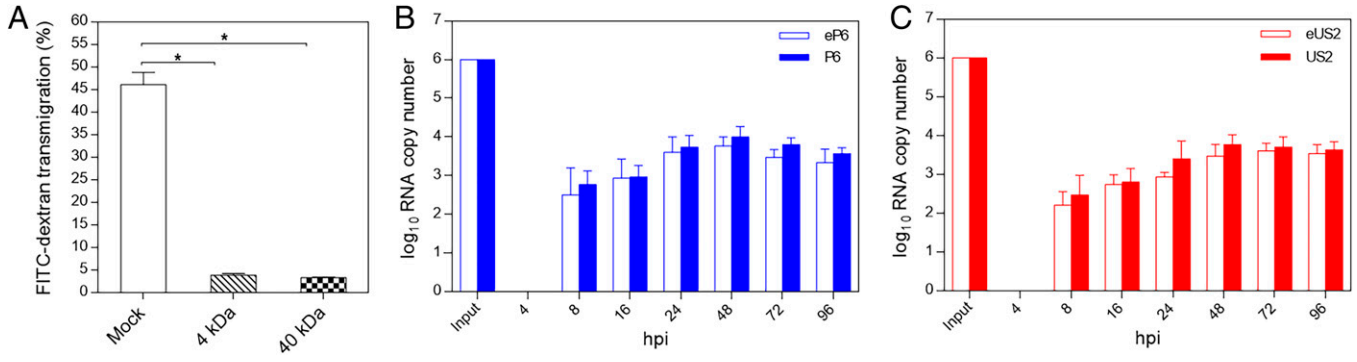

Fig. 2. Establishment of in vitro BBB culture model and demonstration of the ability of quasi-enveloped and nonenveloped HEV virions to cross the BBB. (*A*) The human brain microvascular endothelial cells (hCMEC/D3) were cultured in collagen-coated 0.4-μm PTFE membrane transwell inserts with growth medium for 2 d and then replaced with astrocyte-conditioned media for TJ formation and cultured for 3 d. The FITC-dextran (4 kDa and 40 kDa) were used to test the permeability of the established BBB. Bare PTFE membrane transwell inserts under the same condition were used as the mock control. Each assay was performed in triplicates. *$P < 0.05$, one way ANOVA for statistics analysis. (*B*) Genomic RNA copies (1.0 × 10^6) of eP6 virus or P6 virus were added in the luminal space of the BBB transwell inserts. The culture medium in the abluminal space of the BBB were collected at different time points for quantification of HEV RNAs by qRT-PCR. Each assay was performed in triplicates. (*C*) The quasi-enveloped eUS2 virus and the nonenveloped US2 virus were analyzed using procedures similar to those described in *B*.

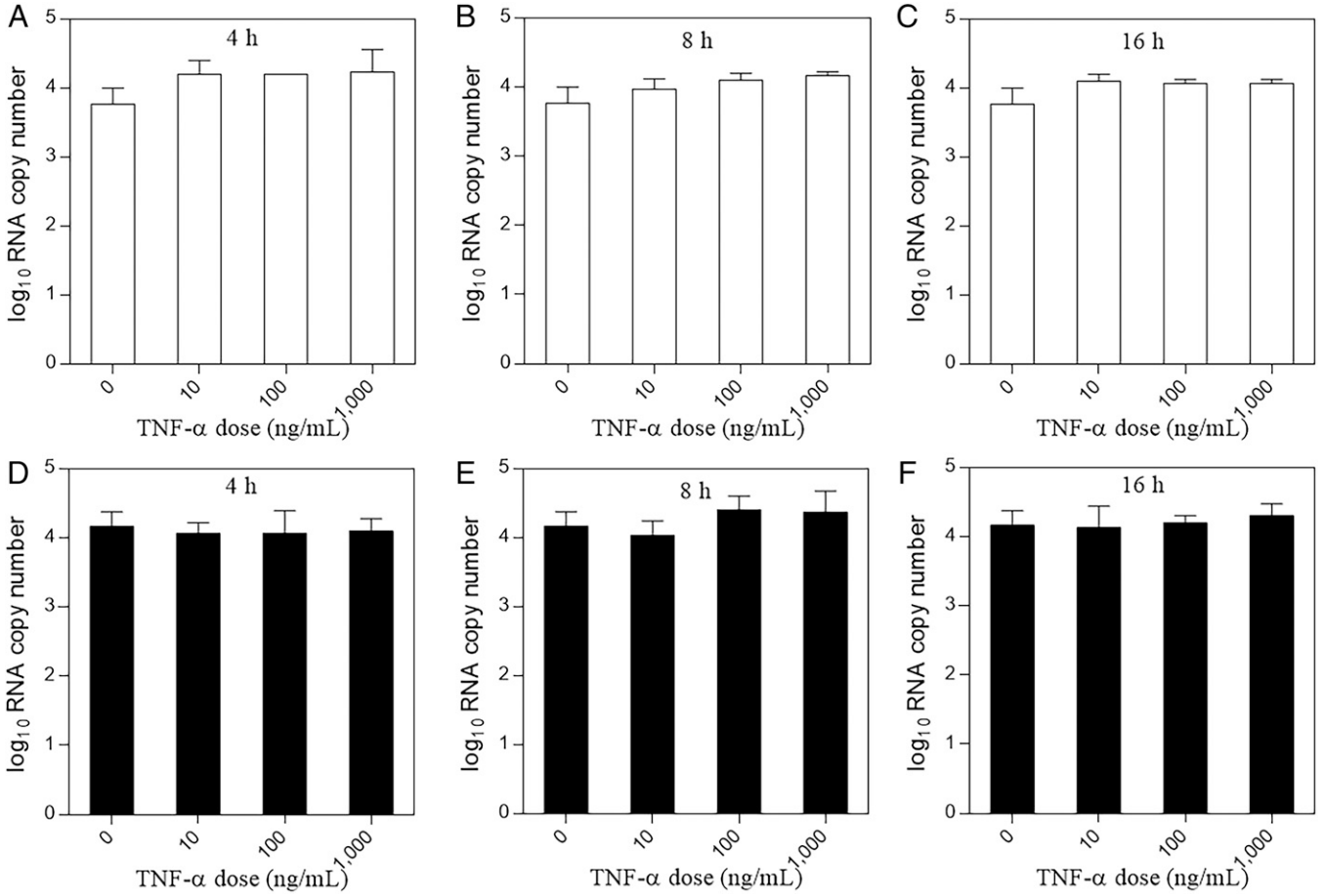

Fig. 3. HEV virions cross the in vitro BBB in a TNF-α–independent manner. The in vitro BBB model was established by growing human brain microvascular endothelial cells (hCMEC/D3) in collagen-coated 0.4-μm PTFE membrane transwell inserts as described in *Materials and Methods*. Prior to HEV infection, the cells were incubated with an increasing dose of TNF-α (0 to 1,000 ng/mL) for different times (4, 8, or 16 h). The cells were washed once with PBS, followed by inoculation with 1.0×10^6 genomic RNA copies of the quasi-enveloped eP6 virus (*A–C*) or with the nonenveloped P6 virus (*D–F*) in the luminal space of the BBB transwell inserts. The medium in the abluminal space of the BBB was collected at 48 hpi for quantification of HEV RNAs. Each assay was performed in triplicates. One-way ANOVA statistics analysis was used.

BBB culture with 1.0×10^6 genomic RNA copies of eP6 or P6 virus, we performed the barrier permeability assay with 40 kDa FITC-dextran. We found that the BBB permeability rate to the 40-kDa FITC-dextran in HEV-infected BBB culture did not significantly increase when compared to mock infection control (Fig. 4*A*). We also quantified the messenger RNA (mRNA) levels by qRT-PCR of selected TJ markers of hCMEC/D3 cells in the BBB culture, which were infected with eP6 or P6 virus for 48 h. We found that the levels of claudin-5, occludin, and VE-C gene expressions in HEV-infected BBB culture did not change significantly when compared to the mock infection control (Fig. 4*B*). The results suggested that the inoculation with quasi-enveloped or nonenveloped HEVs did not significantly disrupt the expression of TJ proteins in the in vitro BBB model, therefore suggesting other potential mechanism(s) for HEV to cross the BBB.

To further investigate the potential mechanism as to how HEV crosses the BBB, we inoculated human brain microvascular endothelial cells (hCMEC/D3), typically lining the BBB in vivo, with eP6 and P6 viruses (1.0×10^6 genomic RNA copies), respectively, for 2 h in a 12-well plate. After washing twice with phosphate-buffered saline (PBS), the cells were cultured in fresh media for 14 d. The amount of HEV RNA in cell culture supernatant at different time points was quantified by qRT-PCR. As shown in Fig. 4*C*, the viral RNAs were detected from 1 d postinoculation (dpi) and lasted for up to 14 d until cell death, and the titer of viral RNA peaked at 6 dpi. To further confirm the observation, we inoculated the hCMEC/D3 cells with a different HEV strain (eUS2 and US2), and similar results were also obtained (*SI Appendix*, Fig. S1*A*). For both virus stains, the viral RNA can be detected as early as 8 hpi.

Furthermore, we also demonstrated that HEV negative-stranded RNA (−) (Fig. 4*D*), which is indicative of virus replication, and viral capsid protein ORF2 at 3 dpi (Fig. 4*E*) were both detected in HEV-infected hCMEC/D3 cells. Additionally, we showed that HEVs also infect human astrocyte CCF-STTG1 (*SI Appendix*, Fig. S1 *C–F*), which is consistent with a previous report (33). The results suggested that HEV virions, both quasi-enveloped and nonenveloped, infect the brain microvascular endothelial cells hCMEC/D3 and astrocyte CCF-STTG1 and cause productive virus infection.

To further confirm that HEV directly enters the brain microvascular endothelial cells forming the in vitro BBB, we tested whether the endocytosis inhibitor 5-(*N*,*N*-hexamethylene) amiloride inhibits HEV entry into cells. As shown in Fig. 4*F*, we demonstrated the inhibition effect of amiloride on eP6 and P6 virus infection of hCMEC/D3 cells. At a concentration of 2.0 mM and above, HEV infection of hCMEC/D3 cells was completely inhibited. We subsequently tested the effect of amiloride on the ability of HEV to cross the in vitro BBB model (Fig. 4*G*) and showed that the amiloride at different concentrations significantly, but not completely even at higher concentrations

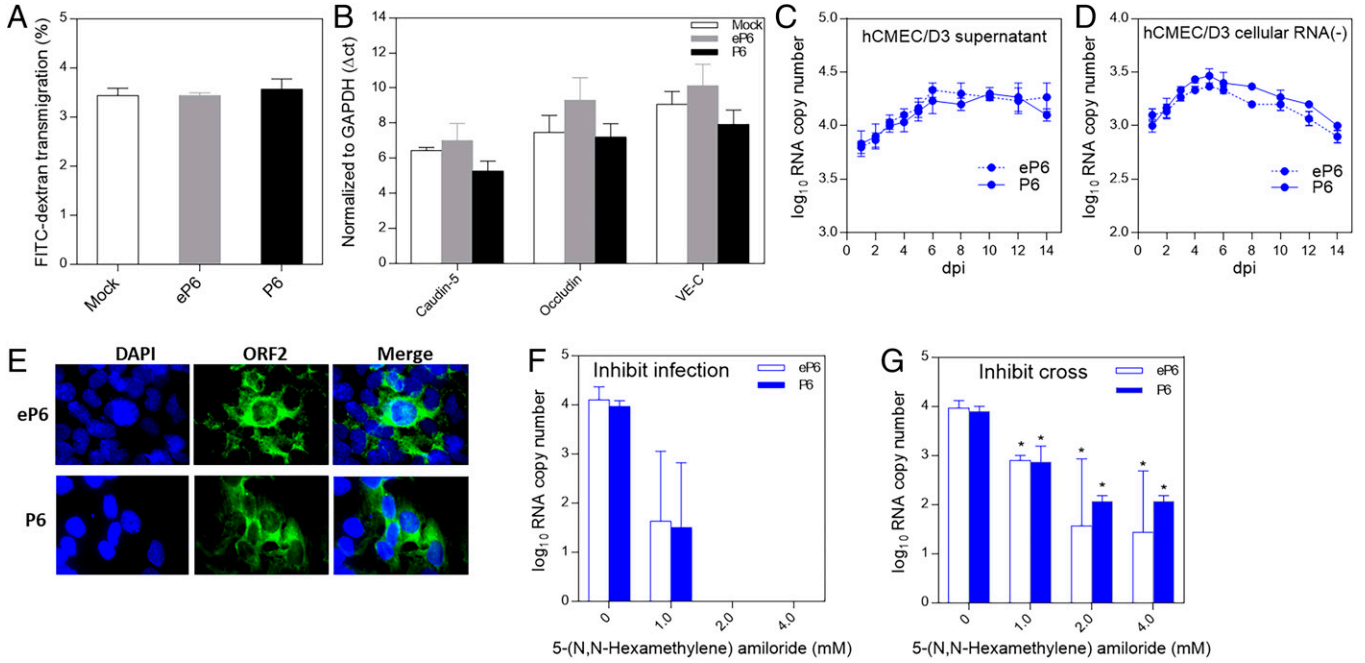

Fig. 4. HEV crosses the in vitro BBB probably via direct infection of brain microvascular endothelial cells. (*A*) Genomic RNA copies (1.0×10^6) of quasi-enveloped eP6 virus or nonenveloped P6 virus or medium only as control were inoculated onto the luminal space of the BBB. At 48 h later, the permeability of the barrier was tested by a permeability assay using 40-kDa FITC-dextran. (*B*) The hCMEC/D3 cells were inoculated with 1.0×10^6 genomic RNA copies of eP6 virus or P6 virus or medium only as control. At 48 h later, cellular RNAs were isolated and the mRNA levels of TJ proteins were quantified by qRT-PCR. The CT values were normalized to GAPDH. The hCMEC/D3 cells in a 12-well plate were inoculated with eP6 or P6 (1.0×10^6) for 2 h. After washing twice, the cells were cultured with medium for 14 d. The culture supernatants (*C*) and cell monolayers (*D*) were collected at indicated time points and subjected to quantification of HEV RNA (*C*) and negative-strand HEV RNA (*D*) by qRT-PCR. (*E*) The hCMEC/D3 cells inoculated with the eP6 virus or P6 virus were stained by IFA using anti-HEV ORF2 antibody at 3 dpi. (*F*) Confluent hCMEC/D3 cells were preinoculated with different concentrations of 5-(*N*,*N*-hexamethylene) amiloride for 30 min. After washing, the cells were inoculated with 1.0×10^6 genomic RNA copies of eP6 or P6 for 2 h and after washing incubated for 48 h. The amounts of HEV RNA in the culture supernatants were quantified by qRT-PCR. (*G*) The in vitro BBB culture inserts were treated with 5-(*N*,*N*-hexamethylene) amiloride, and then HEV virions were added as described in *F*. The amounts of virus crossed into the abluminal space were quantified by qRT-PCR. $^*P < 0.05$, one-way ANOVA.

(2.0 and 4.0 mM), blocked the ability of HEV virions (both eP6 and P6) to cross the barrier. Taken together, the results suggested that direct HEV infection and entry of brain microvascular endothelial cells lining the BBB is a possible mechanism for HEV to cross the BBB.

Both Quasi-Enveloped and Nonenveloped HEVs Invade CNS Tissues in Specific-Pathogen-Free (SPF) Pigs Experimentally Infected with HEV. To investigate whether HEV can cross the BBB in pigs experimentally infected with HEV and whether there is a difference between the quasi-enveloped virus and the nonenveloped virus, SPF pigs were intravenously inoculated with the human-origin genotype 3 HEV quasi-enveloped virus (eUS2) or nonenveloped virus (US2), along with a PBS control group. Fecal virus shedding was detected starting from 3 dpi in one out of seven pigs in the eUS2 group and in seven out of seven pigs in the US2 group (Table 1). All pigs in the US2 group remained positive for HEV RNA in fecal samples until necropsy. For the eUS2 group, all pigs were positive for viral RNA in fecal samples from 7 to 14 dpi but only one pig remained positive for fecal viral RNA at the time of necropsy (Table 1). One out of seven pigs in the eUS2 group and five out of seven pigs in the US2 group were also positive for HEV RNA in serum samples at 14 dpi (Table 1). All pigs in the PBS-inoculated control group remained negative for viral RNA in fecal or serum samples throughout the study. The viral RNA loads in various samples including serum, feces, bile, cerebrospinal fluid (CSF), spinal cord, and brain tissues are shown in *SI Appendix*, Table S2. The results showed that both the quasi-enveloped eUS2 virus and the nonenveloped US2 virus can infect pigs.

To determine whether HEV crosses the BBB and invades CNS tissues, samples of brain and spinal cord were collected at necropsy at 21 dpi and used to detect both positive-stranded (+) and negative-stranded (−) HEV RNA. As shown in Table 1, three of the seven pigs in the US2 group and one of the seven pigs in the eUS2 group were positive for HEV RNA (+) in brain, and one of the seven pigs in the US2 group was positive for HEV RNA (+) in the spinal cord. Negative-strand HEV RNA, an indication of virus replication, was also detected in the brain tissues from two of the three pigs with detectable HEV RNA (+) in the brains (Table 1). The viral RNA loads in these positive brain and spinal cord samples were $\sim 1.0 \times 10^5$ per g of tissue (*SI Appendix*, Table S2).

To further verify the presence of HEV RNA in brain and spinal cord, we performed fluorescence in situ hybridization (FISH) by using an HEV ORF2 gene-specific probe to detect viral RNA in brain and spinal cord. The results from the FISH data showed that, in the CNS tissues with detectable viral RNA, two out of three brains and one spinal cord had a positive HEV RNA in situ hybridization signal (Fig. 5*A*). This result further confirmed the presence of HEV RNAs in these CNS tissues. No viral RNA was detected in the CSF collected at 3 dpi in any of the pigs, although the CSF from one pig at 21 dpi in the US2 group was positive for HEV RNA (Table 1).

Collectively, these data clearly demonstrated that HEVs, both quasi-enveloped and nonenveloped virions, were able to invade CNS tissues in pigs experimentally infected with genotype 3 HEV.

Table 1. Detection of HEV RNA in various samples from pigs experimentally infected with the membrane-associated quasi-enveloped eUS2 virus and the nonenveloped US2 virus

		Serum				Feces						Bile	CSF		Spinal cord (+)/(−)*	Brain (+)/(−)
Group	No. of pigs	0 dpi	7	14	21	0	3	7	10	14	21	21	3	21	21	21
Control	7	0†	0	0	0	0	0	0	0	0	0	0	0	0	0/0	0/0
eUS2	7	0	0	1	0	0	1	7	7	7	1	3	0	0	0/0	1/0
US2	7	0	2	5	3	0	7	7	7	7	7	6	0	1	1/0	3/2

*(+): positive-strand HEV RNA; (−): negative-strand HEV RNA.
†Number of HEV RNA-positive pigs at days post inoculation.

HEV Infection Causes Histological Lesions in CNS Tissues and Induces Higher Serum Levels of Proinflammatory Cytokines TNF-α and Interleukin (IL) 18. Since HEV was detected in the CNS of a proportion of the infected pigs, we examined the histopathological lesions in the CNS tissues in all HEV-infected and control pigs. Mild brain histological changes including meningitis, perivascular inflammation, and gliosis were observed in two of the three pigs with detectable HEV RNAs in brain tissues (Fig. 5*B*). Severe perivascular inflammation and gliosis were also observed in the spinal cord from the only pig with detectable HEV RNAs in the spinal cord tissue. (Fig. 5*B*). The results suggested that HEV invasion of the CNS caused histopathological lesions in only a proportion of infected animals. Under the experimental condition and the animal model used in the study, we did not observe any neurological symptom in any of the HEV-infected pigs.

HEV infection is known to induce proinflammatory cytokines which could facilitate HEV entry into the CNS. Therefore, in this study we also measured the serum levels of proinflammatory cytokines including TNF-α and IL-18. As shown in Fig. 5*C*, the serum level of TNF-α started to increase at 14 dpi in both eUS2 and US2 virus-inoculated groups, and the pigs in the US2 group had a significantly higher serum level of TNF-α than that in other groups at 21 dpi. The results confirmed that the HEV (US2 strain) infection induced a high level of proinflammatory cytokine TNF-α in pigs.

When we performed further analysis of TNF-α level in individual pigs from the US2 virus-infected group at 21 dpi, we found that pigs with detectable HEV RNAs in CNS tissues ($n = 3$) had significantly higher serum levels of TNF-α than pigs with no detectable HEV RNA in CNS tissues ($n = 4$) (Fig. 5*D*). Similar results were also found for serum levels of IL-18, another proinflammatory cytokine (Fig. 5 *E* and *F*). The three pigs which were positive for HEV in brains and had higher levels of TNF-α /IL-18 did not correlate with higher virus loads in infected pigs. The results suggested that the proinflammatory cytokines produced during HEV infection might play a role in HEV-associated neurological disorders, although the underlying mechanism is unknown.

We also quantified the mRNA levels of selected TJ proteins from pig brain tissues. We showed that pig brain tissues in the eUS2 and US2 viruses-inoculated groups had slightly lower

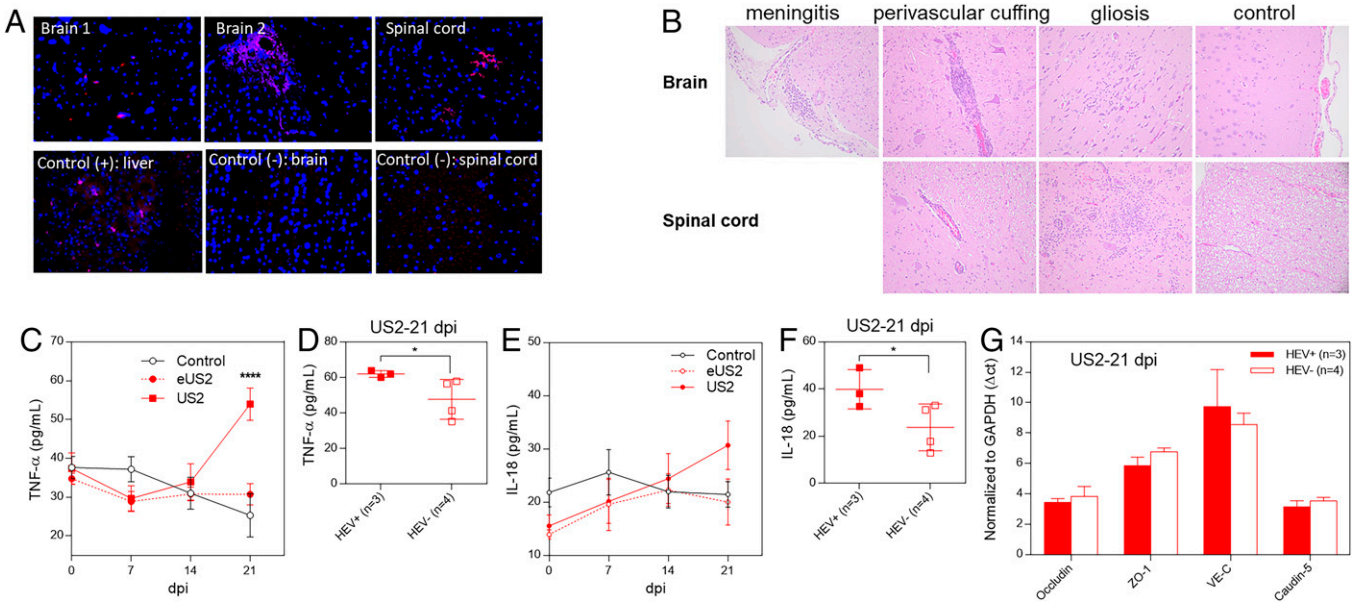

Fig. 5. HEV invades the CNS tissues in HEV-infected pigs. Four-week-old HEV-negative SPF pigs were intravenously inoculated with the quasi-enveloped eUS2 virus or nonenveloped US2 or medium as control. Samples of brain and spinal cord were collected at 21 dpi. (*A*) The formalin-fixed tissues of brains and spinal cords were paraffin-embedded and in situ-hybridized with a fluorescent-labeled (red) HEV-specific probe (representative pictures showing the detection of HEV RNAs in CNS tissues by FISH are shown). (*B*) The tissues of brains and spinal cords were H&E-stained and paraffin-embedded. The histological lesions were evaluated, in a blind fashion, by a board-certified veterinary pathologist (T. L.). Representative histopathology pictures are shown. Weekly sera were collected from each infected pig and the serum levels of TNF-α (*C*) and IL-18 (*E*) were determined. Comparison of the serum levels of TNF-α (*D*) and IL-18 (*F*) between HEV-infected pigs with detectable HEV RNAs in brain tissues ($n = 3$) and infected pigs with no detectable HEV RNA in brain tissues ($n = 4$) at 21 dpi. (*G*) Total RNAs were isolated from the brain tissues of the US2-infected pigs at 21 dpi. The mRNA levels of the TJ proteins in brain tissues (occludin, ZO-1, VE-C, and caudin-5) were quantified by qRT-PCR. *$P < 0.05$, ****$P < 0.0001$, one-way ANOVA.

levels of occludin and VE-C mRNAs than those in the control group, but the difference was not statistically significant. In the US2 group, only VE-C was slightly, but not significantly, lower in the three pigs with detectable HEV RNAs in CNS tissues than those in the four pigs with no detectable HEV in CNS tissues (Fig. 5*G*).

Discussion

In addition to causing acute and chronic viral hepatitis, HEV infection has also been associated with a number of extrahepatic manifestations including various neurological sequelae, which has increasingly become a significant clinical problem (48). The neurological disorders associated with HEV infection include Guillain–Barré syndrome, neuralgic amyotrophy, encephalitis, and myelitis, among others (20, 22, 49). The mechanism of HEV-associated neuroinvasion and how HEV causes neurological injury remain unknown. One potential mechanism is that HEV directly infects nervous cells, causing neural cell injury, as HEV has been reported to replicate in various human neuronal-derived cell lines (33). HEV was also reportedly detected in brain tissues from mice and monkeys experimentally infected with HEV and in CSF from patients with HEV-associated neurological disorders (31). These studies supported a hypothesis that HEV causes neurological damage via direct infection of nervous cells in the CNS, but how HEV gains access to the CNS is unknown.

In the present study, we first established and utilized an in vitro BBB culture model to investigate the possible mechanism(s) of HEV-associated neuroinvasion. Our data showed that HEV can cross the in vitro BBB without significantly altering the TJ proteins of the BBB. The results from the BBB permeability assay also revealed that HEV did not significantly increase the in vitro BBB permeability rate. The detection of HEV RNA in the abluminal space at 8 hpi is intriguing for HEV. In addition to transcytosis, which may transmit some viruses to the abluminal space, another potential explanation is the limitation of the in vitro BBB culture model as a small amount of molecules could still pass through the in vitro BBB. However, this observation was consistent with our finding in the HEV infection assay showing that HEV RNA was detected at 8 hpi, and there are also publications reporting the detection of HEV RNAs in infected cells as early as 4 hpi (50, 51). We subsequently conducted an experimental HEV infection study in SPF pigs and showed that, in pigs experimentally infected with HEV, there is no significant down-regulation of TJ protein gene expression levels in pigs with detectable HEV RNAs in brain and spinal cord tissues. Taken together, our in vitro and in vivo results suggest that HEV may utilize other mechanism(s) to gain access to and invade CNS.

The in vitro BBB culture model consists of mainly the human brain microvascular endothelial cells (hCMEC/D3) that form the TJ in the BBB. Therefore, we next tested whether the brain microvascular endothelial cells forming the in vitro BBB are susceptible to HEV infection. Interestingly, we found that HEV can productively infect the brain microvascular endothelial cells. We demonstrated that, in hCMEC/D3 cells inoculated with HEV, extracellular viral genomic RNA, intracellular negative-stranded HEV RNA, and intracellular HEV capsid protein were all detected. Furthermore, we showed that HEV infection of hCMEC/D3 cells is inhibited by the endocytosis inhibitor 5-(*N*,*N*-hexamethylene) amiloride. Additionally, consistent with a previous report (33), we found that astrocytes can be productively infected by HEV as well.

Based on our results in this study and additional evidence from two other reports (31, 33), we proposed a possible mechanism of HEV neuroinvasion: HEV invades CNS via direct infection of brain microvascular endothelial cells and subsequently infects neuronal cells to cause injury in CNS tissues. This potential mechanism has been observed in several other viruses. For example, measles virus, mouse adenovirus 1, and Epstein–Barr virus can all infect brain microvascular endothelial cells to invade the CNS (52–55). It should be noted here that direct HEV infection of brain microvascular endothelial cells is probably an important, but not the only, mechanism for HEV-associated neuroinvasion. Other potential mechanisms, such as BBB breakdown, or retrograde transport of virus from peripheral nerves to the CNS, may also be used by neurotropic viruses separately or in combination (54, 56). Therefore, although our results from this study suggest a possible mechanism of HEV-associated neuroinvasion, we cannot completely rule out other potential mechanisms at this point.

Exosomes are extracellular membrane-enclosed microvesicles which play a role in intercellular signaling (57). Exosomes can relatively freely migrate across biological membranes, including the BBB (58, 59). HEV virions in the circulating blood are membrane-associated quasi-enveloped particles resembling exosomes, and therefore we investigated whether the exosome-like quasi-enveloped HEV virions can facilitate virus entry across the BBB (31, 41). Our data showed that both the exosome-like quasi-enveloped HEV and the nonenveloped HEV can cross the BBB in similar time courses, thus suggesting that the exosome-like quasi-enveloped HEV does not appear to have a significant advantage for crossing the BBB. Our in vivo HEV infection study in pigs also confirmed the in vitro findings, as we found that the nonenveloped US2 virus was also able to invade the CNS tissues in infected pigs. The quasi-enveloped HEV virions lack viral protein on the surface, but they can still enter the host cells via a clathrin-mediated endocytosis, although this process is generally less efficient compared to nonenveloped HEV virions (40). A lower virus titer used for virus inoculation in pigs and the inherited less-efficient endocytosis of the quasi-enveloped HEV might contribute to the observation in this study that the quasi-enveloped eUS2 virus replicates less efficiently in pigs compared to the nonenveloped US2, since only one pig in the eUS2 group had detectable HEV RNAs in the CNS tissues. Therefore, it is possible that, even if the exosome-like quasi-enveloped HEVs do play a role in HEV entry into BBB, direct HEV infection of brain microvascular endothelial cells and subsequent infection of neuronal cells are probably more important for HEV neuroinvasion.

TNF-α is a proinflammatory cytokine which is capable of disrupting TJ and enhancing BBB permeability (60). By using an in vitro BBB culture model, surprisingly we found that HEV crossed the BBB in a TNF-α–independent manner: Inoculation of the in vitro barrier with TNF-α prior to HEV infection did not significantly increase the amount of HEV that crossed the barrier. Again, this finding could be explained by the proposed possible mechanism of direct HEV infection of cells lining the BBB. However, in our in vivo HEV infection study in pigs we found that HEV-infected pigs with detectable HEV RNAs in CNS tissues had a significantly higher serum level of TNF-α than that in HEV-infected pigs with no detectable HEV RNA in CNS tissues. There was no significant difference in the mRNA levels of TJ proteins in brain tissues between infected pigs with detectable HEV RNAs in CNS and infected pigs with no detectable HEV RNA in the CNS. Further in-depth experiments are warranted to more definitively

determine whether the relatively high level of TNF-α produced during HEV infection can enhance BBB permeability and promote HEV neuroinvasion in vivo.

In addition to TNF-α, a significantly elevated level of the proinflammatory cytokine IL-18 was also detected in HEV-infected pigs with detectable HEV RNAs in CNS tissues. An elevated level of these proinflammatory cytokines hinted that the occurrence of neuroinflammation in CNS tissues could be one of the pathogenic processes for HEV-associated neurological injury (61, 62). In this study, we did observe histological lesions such as meningitis, perivascular inflammation, and gliosis in the brain and spinal cord of HEV-infected pigs with detectable viral RNAs in CNS tissues, thus suggesting that neuroinflammation might play a role in HEV-associated neurological injury. Therefore, future experiments are warranted to further investigate whether HEV, like other viruses such as HIV and severe acute respiratory syndrome coronavirus 2, induce neurological damages via induction of neuroinflammation (63, 64).

In summary, by using an in vitro BBB culture model and in vivo HEV infection study in pigs we demonstrated that HEV virions, both quasi-enveloped and nonenveloped, were able to cross the BBB and invade the CNS. We also demonstrated that both forms of HEV virions productively infect brain microvascular endothelial cells forming the in vitro BBB. The results from this study led us to propose a possible mechanism of HEV-associated neuroinvasion in which HEV gains access to and invades the CNS via direct infection of brain microvascular endothelial cells lining the BBB. Future studies are warranted to understand why only a small number of infected animals had detectable HEV in CNS tissues, which is also consistent with the clinical presentation of neurological disorders only in a small population of HEV-infected human patients. The results from this study shed light on understanding the mechanism of HEV-associated neurological disorders and highlight the critical need of a HEV-specific antiviral to treat HEV-related neurological sequelae.

Materials and Methods

Cells and Viruses. A subclone of the human hepatoma Huh7 cell line, Huh7-S10-3, a gift from Suzanne U. Emerson, NIH, Bethesda, MD, was used for generating infectious HEV RNA for transfection in this study. Another human hepatoma cell line, HepG2, was purchased from ATCC and used to propagate HEV. Both cell lines were maintained in Dulbecco's modified Eagle's medium (DMEM) with 10% fetal bovine serum (FBS) at 37 °C with 5% CO_2. A human astrocyte-derived cell line (CCF-STTG1) was purchased from ATCC and cultured in DMEM with 10% FBS. A human brain microvascular endothelial cell line (hCMEC/D3), which is derived from human temporal lobe microvessel endothelial cells (Millipore, SCC066), was cultured in a collagen-coated flask or plate with hCMEC/D3-specific EndoGRO-MV complete media (Millipore, SCME004) containing human fibroblast growth factor (65). Genotype 3 HEV strain Kernow-C1/P6 (designated as P6) was rescued by transfection of Huh7-S10-3 cells with in vitro-transcribed RNAs from an infectious complementary DNA (cDNA) clone of the HEV P6 strain (66). The virus stock of another human-origin genotype 3 HEV (strain US2) was prepared in 10% PBS suspension of feces from experimentally infected pigs (67).

Generation of Membrane-Associated Quasi-Enveloped and Nonenveloped HEV Virions. Full-length capped genomic RNA transcripts from an HEV P6 infectious clone were transfected into Huh7-S10-3 cells in a six-well plate using DMRIE-C reagent (Invitrogen) according to the manufacturer's instructions. The transfected cells were cultured in DMEM maintenance medium with 4% FBS at 34.5 °C. Approximately 3 d after transfection, the cell monolayer was detached by treatment with 2.5% trypsin–ethylenediaminetetraacetic acid. DMEM maintenance medium was subsequently added to the suspended cells, which were then transferred into a T75 flask (8.0×10^4 cells per cm^2). Cells in the flask were cultured for 15 d. Half of the culture supernatant was collected and fresh medium was replaced into flask every 3 d. The collected culture supernatants were pooled and subjected to ultracentrifugation at 100,000 × *g* for 2 h at 4 °C. The pellet was resuspended with PBS and stored at −80 °C as the virus stock of membrane-associated quasi-enveloped P6 (eP6) virions.

To produce the nonenveloped HEV virions, the HEV eP6 virions were treated with 0.1% DOC-Na and trypsin for 5 h at 37 °C to remove the quasi-envelope. The treated virus was diluted with PBS and then subjected to ultracentrifugation as described above. The pellet was resuspended with PBS and stored at −80 °C as the virus stock of nonenveloped HEV P6 (P6) virions.

The human-origin genotype 3 HEV (stain US2) stock prepared in 10% fecal suspension was first centrifuged (3,000 × *g*) to remove the debris and then filtrated through 0.2-μm filter. The filtrate was stored at −80 °C as the virus stock of the nonenveloped HEV US2 (US2) virions. The membrane-associated quasi-enveloped HEV US2 (eUS2) was generated by experimental infection of the HepG2 cells with the US2 virus. Briefly, the US2 virus was inoculated onto the HepG2 cells at 70% confluency and incubated at 37 °C for 2 h. After washing twice with PBS, cells were cultured with DMEM containing 4% low-immunoglobulin G FBS, 2.5 μg/mL amphotericin B, and 2× antibiotics at 34.5 °C (50). Every 5 d, half of the culture supernatant was collected and then replaced with fresh medium until 25 dpi. The collected culture supernatants were pooled and subjected to ultracentrifugation as described similarly for HEV eP6. The pellet was resuspended with PBS and stored at −80 °C as the HEV eUS2 virus stock.

Sucrose Density Gradient Centrifugation. Viruses were first ultraconcentrated at 100,000 × *g* for 2 h at 4 °C using Beckman SW28 rotor. The pellets were then resuspended with PBS and loaded on a gradient-density sucrose (10 to 70%) for ultracentrifugation at 120,000 × *g* for 18 h at 4 °C using SW41 rotor. A total of 20 fractions were collected and the density of each fraction was measured.

Immunoblotting. Concentrated viruses were loaded with loading buffer and inactivated at 95 °C for 5 min. After separation via sodium dodecyl sulfate polyacrylamide gel electrophoresis, proteins were transferred to nitrocellulose membrane for immunoblotting analysis. The anti-CD63 monoclonal antibody (mAb) anti-Rab27 mAb (Santa Cruz Biotechnology) and anti-HEV ORF2 mAb (Millipore-Sigma) were used for the immunoblotting assay. Protein bands were visualized by an Odyssey imaging system (LI-COR Biosciences).

Establishing the BBB In Vitro Culture Model. The supernatant from 100% confluence of astrocyte cell culture was collected and centrifuged to remove any cellular debris and subsequently mixed with hCMEC/D3 complete media (50% vol/vol) to produce the astrocyte-conditioned media for TJ formation. The hCMEC/D3 cells were seeded on collagen-coated 0.4-μm PTFE membrane transwell inserts (5.0×10^4 cells per cm^2) and cultured in the hCMEC/D3 complete media at 37 °C with 5% CO_2 for about 2 d to 90% confluence. The media was subsequently replaced with astrocyte-conditioned media and cultured for 3 d to form TJ. To determine the integrity of the in vitro BBB, the FITC-dextran permeability assay was conducted as described elsewhere (68). Briefly, after 5-d culture, 4-kDa or 40-kDa FITC-dextran (Sigma, 100 μg/mL) were added into the upper chamber (luminal space) of the transwell inserts. One hour later, the media in the lower chamber (abluminal space) was collected and subjected to fluorescence reading. Bare transwell insert under the same condition was used as the mock control. To determine the expression of TJ proteins, hCMEC/D3 cells were seeded on four-well cell culture slides. The seeding density and culture condition were the same as described in the transwell insert. The TJ marker proteins of ZO-1, Gai2, occludin, and claudin-5 were stained via IFA using marker-specific antibodies.

IFA. The cells were fixed with 4% paraformaldehyde at room temperature for 30 min, permeabilized with 0.2% Triton-100 at room temperature for 30 min, and blocked with 1% bovine serum albumin at 37 °C for 30 min. Subsequently, the cells were incubated with each of the specific primary antibodies, respectively, at 37 °C for 2 h. After washing with PBS three times, the cells were incubated with respective fluorescence-conjugated secondary antibodies (Molecular Probes) at 37 °C for 1 h and subsequently washed three times with PBS. Cell nuclei were

counterstained with DAPI. Cells were viewed under a fluorescence microscopy using 40× or 100× lens.

In Vitro Assay to Assess Whether HEV Crosses the BBB. The in vitro BBB culture was washed with PBS twice. Quasi-enveloped HEV or nonenveloped HEV were each added into luminal space. To remove the potential effect of exosome which is derived from culture media, we used exosome-free FBS (Sigma) in the culture media for nonenveloped HEV virions. The BBB cultures were incubated at 37 °C. At indicated different time points postinoculation, the culture media in abluminal space were collected and subjected to quantification of HEV RNA.

To test the effect of TNF-α stimulation on the ability of HEV to cross the BBB, the BBB culture was washed with PBS and subsequently incubated with different concentrations of TNF-α for different time periods (4, 8, or 16 h). The BBB culture was washed once with PBS, and then 1.0×10^6 genomic RNA copies of quasi-enveloped or nonenveloped HEV virions were added into the luminal space of the transwell inserts. After 48-h incubation, the media in abluminal space were collected for quantification of HEV RNA.

Experimental Infection of SPF Pigs with Quasi-Enveloped and Nonenveloped HEV Virions. Approximately 4-wk-old, HEV-seronegative, SPF pigs were divided into three groups (groups 1 to 3) with seven pigs per group. Each group of pigs was housed separately in a BSL-2 swine research facility. The pigs in group 1 were each intravenously inoculated with PBS as control, group 2 each with 2.0×10^7 RNA copy of quasi-enveloped HEV eUS2, and group 3 each with 1.0×10^8 RNA copy of nonenveloped HEV US2. Fecal and serum samples were collected prior to inoculation and weekly thereafter from each pig to detect HEV RNAs. At 3 dpi, samples of CSF were collected from each pig via cisterna magna centesis with a spinal needle under general anesthesia. At 21 dpi, samples of CSF were similarly collected again from each pig prior to necropsy. During necropsy, samples of brain and spinal cord were collected and immediately stored at −80 °C. Also, an aliquot of brain and spinal cord tissues was fixed in 10% formalin and stained by hematoxylin/eosin (H&E) for routine histological examination, in a blind fashion, by a board-certified veterinary pathologist. Liver and bile samples were collected at necropsy as well. The animal study was approved by the Institutional Animal Care and Use Committee at Virginia Polytechnic Institute and State University (approval number IACUC-18-169).

RNA Extraction. HEV viral RNAs were extracted from cell culture supernatants or pig serum using Viral RNA kit (Zymo Research) according to the manufacturer's instructions. For the cultured cells, total cellular RNAs were isolated using TRI Reagent (Zymo Research). For the pig tissues, the samples were first homogenized and resuspended in 10% PBS before RNA extraction. The fecal samples were also resuspended in 10% PBS. After removal of solid debris by centrifugation, the supernatants were used to extract the total RNAs using TRI Reagent.

qRT-PCR and Nested RT-PCR. HEV genomic RNA (+) was quantified via one-step qRT-PCR using the Bioline Sensifast Probe No Rox One-Step Kit (Thomas Scientific). The primers, probe, and protocol have been described elsewhere (69). The in vitro-transcribed genomic RNA from the infectious clone of HEV P6 was used as the standard. The HEV negative-stranded RNA (−) was quantified by using a two-step qRT-PCR. The cDNAs were synthesized from total RNAs using the SuperScript IV First-Strand Synthesis System (Invitrogen). The synthesized cDNAs were then used for qPCR analysis using iTaq universal probe kit (Bio-Rad). The nested RT-PCR was conducted using an established protocol described elsewhere (70). The primers and probe information are listed in *SI Appendix*, Table S1.

Quantification of TJ Protein mRNAs by qRT-PCR. The total RNAs were isolated from tissue samples as described above. One-step qRT-PCR assay was conducted using an iTaq Universal SYBR Green One-Step Kit (Bio-Rad). The primers, which were used to amplify genes of pig GAPDH, occludin, ZO-1, VE-cadherin (VE-C), and claudin-5, are listed in *SI Appendix*, Table S1.

Cytokine Assays to Measure TNF-α and IL-18. Commercial kits were used to quantitatively determine the levels of pig TNF-α (Quantikine ELISA Porcine TNF-α; R&D Systems) and IL-18 (Porcine IL-18 ELISA Kit; MyBioSource) in sera of HEV-infected and control pigs according to the manufacturer's instructions.

FISH Assay. The FISH assay was performed on formalin-fixed, paraffin-embedded CNS tissue sections to detect HEV RNAs. The in vitro-transcribed RNA probe was specific for the HEV ORF2 and labeled with fluorescent dyes by using a FISH tag RNA multicolor kit (Invitrogen, F32956) according to the protocols provided in the commercial kit. The CNS tissue sections were visualized under a fluorescence microscopy using 40× lens.

Data Availability. All study data are included in the article and/or *SI Appendix*.

ACKNOWLEDGMENTS. We thank Cassandra Fields, Rachel McNeil, Karen Hall, and the staff in the Laboratory Animal Resources at Virginia Polytechnic Institute and State University for their help in the animal study. We thank Drs. Suzanne U. Emerson and Robert H. Purcell at the NIH, Bethesda, MD for kindly providing us with the Huh7-S10-3 cells. This study is supported by NIH grants R21AI141677 and R01AI050611. X.-J.M. was the principal investigator and W.L. was co-principal investigator on the grant.

Author affiliations: [a]Department of Biomedical Sciences and Pathobiology, Virginia–Maryland College of Veterinary Medicine, Virginia Polytechnic Institute and State University, Blacksburg, VA 24061; [b]Center for Emerging, Zoonotic and Arthropod-Borne Pathogens, Fralin Life Sciences Institute, Virginia Polytechnic Institute and State University, Blacksburg, VA 24061; and [c]Department of Large Animal Clinical Sciences, Virginia–Maryland College of Veterinary Medicine, Virginia Polytechnic Institute and State University, Blacksburg, VA 24061

1. B. Wang, X. J. Meng, Hepatitis E virus: Host tropism and zoonotic infection. *Curr. Opin. Microbiol.* **59**, 8–15 (2021).
2. I. Nimgaonkar, Q. Ding, R. E. Schwartz, A. Ploss, Hepatitis E virus: Advances and challenges. *Nat. Rev. Gastroenterol. Hepatol.* **15**, 96–110 (2018).
3. D. B. Rein, G. A. Stevens, J. Theaker, J. S. Wittenborn, S. T. Wiersma, The global burden of hepatitis E virus genotypes 1 and 2 in 2005. *Hepatology* **55**, 988–997 (2012).
4. Y. Geng *et al.*, High seroprevalence of hepatitis E virus in rabbit slaughterhouse workers. *Transbound. Emerg. Dis.* **66**, 1085–1089 (2019).
5. Y. Nan, C. Wu, Q. Zhao, E. M. Zhou, E. Zoonotic Hepatitis, Zoonotic hepatitis E virus: An ignored risk for public health. *Front. Microbiol.* **8**, 2396 (2017).
6. H. R. Dalton, R. Bendall, S. Ijaz, M. Banks, E. Hepatitis, Hepatitis E: An emerging infection in developed countries. *Lancet Infect. Dis.* **8**, 698–709 (2008).
7. X. J. Meng *et al.*, A novel virus in swine is closely related to the human hepatitis E virus. *Proc. Natl. Acad. Sci. U.S.A.* **94**, 9860–9865 (1997).
8. X. J. Meng, Expanding host range and cross-species infection of hepatitis E virus. *PLoS Pathog.* **12**, e1005695 (2016).
9. S. Sridhar *et al.*, Transmission of rat hepatitis E virus infection to humans in Hong Kong: A clinical and epidemiological analysis. *Hepatology* **73**, 10–22 (2020).
10. A. Andonov *et al.*, Rat hepatitis E virus linked to severe acute hepatitis in an immunocompetent patient. *J. Infect. Dis.* **220**, 951–955 (2019).
11. C. Cangin, B. Focht, R. Harris, J. A. Strunk, Hepatitis E seroprevalence in the United States: Results for immunoglobulins IGG and IGM. *J. Med. Virol.* **91**, 124–131 (2019).
12. P. Rawla *et al.*, A systematic review of the extra-hepatic manifestations of hepatitis E virus infection. *Med. Sci. (Basel)* **8**, 9 (2020).
13. B. Wang *et al.*, Identification of a novel hepatitis E virus genotype 3 strain isolated from a chronic hepatitis E virus infection in a kidney transplant recipient in Switzerland. *Genome Announc.* **5**, e00345-17 (2017).
14. N. F. Crum-Cianflone *et al.*; Infectious Disease Clinical Research Program HIV Working Group, Hepatitis E virus infection in HIV-infected persons. *Emerg. Infect. Dis.* **18**, 502–506 (2012).
15. U. Navaneethan, M. Al Mohajer, M. T. Shata, Hepatitis E and pregnancy: Understanding the pathogenesis. *Liver Int.* **28**, 1190–1199 (2008).
16. N. Kamar *et al.*, Hepatitis E virus and neurologic disorders. *Emerg. Infect. Dis.* **17**, 173–179 (2011).
17. N. Kamar, S. Pischke, Acute and persistent hepatitis E virus genotype 3 and 4 infection: Clinical features, pathogenesis, and treatment. *Cold Spring Harb. Perspect. Med.* **9**, a031872 (2019).
18. O. Marion *et al.*, Hepatitis E virus-associated cryoglobulinemia in solid-organ-transplant recipients. *Liver Int.* **38**, 2178–2189 (2018).
19. D. Guinault *et al.*, Hepatitis E virus-induced cryoglobulinemic glomerulonephritis in a nonimmunocompromised person. *Am. J. Kidney Dis.* **67**, 660–663 (2016).
20. O. Stevens, K. G. Claeys, K. Poesen, V. Saegeman, P. Van Damme, Diagnostic challenges and clinical characteristics of hepatitis E virus-associated Guillain-Barré syndrome. *JAMA Neurol.* **74**, 26–33 (2017).
21. F. Abravanel *et al.*; HEV study group, Acute hepatitis E in French patients and neurological manifestations. *J. Infect.* **77**, 220–226 (2018).
22. H. R. Dalton *et al.*, Hepatitis E virus and neurological injury. *Nat. Rev. Neurol.* **12**, 77–85 (2016).
23. K. Mandal, N. Chopra, Acute transverse myelitis following hepatitis E virus infection. *Indian Pediatr.* **43**, 365–366 (2006).
24. A. K. Jha, G. Kumar, V. M. Dayal, A. Ranjan, A. Suchismita, Neurological manifestations of hepatitis E virus infection: An overview. *World J. Gastroenterol.* **27**, 2090–2104 (2021).
25. H. R. Dalton *et al.*, Hepatitis E virus infection and acute non-traumatic neurological injury: A prospective multicentre study. *J. Hepatol.* **67**, 925–932 (2017).
26. Y. Wang *et al.*, Hepatitis E virus infection in acute non-traumatic neuropathy: A large prospective case-control study in China. *EBioMedicine* **36**, 122–130 (2018).

27. M. Fritz-Weltin *et al.*, Acute CNS infections - Expanding the spectrum of neurological manifestations of hepatitis E virus? *J. Neurol. Sci.* **423**, 117387 (2021).
28. P. Ripellino *et al.*, Neurologic complications of acute hepatitis E virus infection. *Neurol. Neuroimmunol. Neuroinflamm.* **7**, e643 (2019).
29. M. Fraga *et al.*, Hepatitis E virus as a cause of acute hepatitis acquired in Switzerland. *Liver Int.* **38**, 619–626 (2018).
30. R. Shi *et al.*, Evidence of hepatitis E virus breaking through the blood-brain barrier and replicating in the central nervous system. *J. Viral Hepat.* **23**, 930–939 (2016).
31. X. Zhou *et al.*, Hepatitis E virus infects neurons and brains. *J. Infect. Dis.* **215**, 1197–1206 (2017).
32. J. Tian *et al.*, Brain infection by hepatitis E virus probably via damage of the blood-brain barrier due to alterations of tight junction proteins. *Front. Cell. Infect. Microbiol.* **9**, 52 (2019).
33. S. A. Drave *et al.*, Extra-hepatic replication and infection of hepatitis E virus in neuronal-derived cells. *J. Viral Hepat.* **23**, 512–521 (2016).
34. D. B. Smith *et al.*; Members of The International Committee On The Taxonomy Of Viruses Study Group, Consensus proposals for classification of the family Hepeviridae. *J. Gen. Virol.* **95**, 2223–2232 (2014).
35. D. B. Smith *et al.*, Update: Proposed reference sequences for subtypes of hepatitis E virus (species *Orthohepevirus A*). *J. Gen. Virol.* **101**, 692–698 (2020).
36. F. Yang *et al.*, Current status of hepatitis E virus infection at a rhesus monkey farm in China. *Vet. Microbiol.* **230**, 244–248 (2019).
37. S. P. Kenney, X. J. Meng, Hepatitis E virus genome structure and replication strategy. *Cold Spring Harb. Perspect. Med.* **9**, a031724 (2019).
38. X. Yin *et al.*, Origin, antigenicity, and function of a secreted form of ORF2 in hepatitis E virus infection. *Proc. Natl. Acad. Sci. U.S.A.* **115**, 4773–4778 (2018).
39. Q. Ding *et al.*, Hepatitis E virus ORF3 is a functional ion channel required for release of infectious particles. *Proc. Natl. Acad. Sci. U.S.A.* **114**, 1147–1152 (2017).
40. X. Yin, C. Ambardekar, Y. Lu, Z. Feng, Distinct entry mechanisms for nonenveloped and quasi-enveloped hepatitis E viruses. *J. Virol.* **90**, 4232–4242 (2016).
41. S. Nagashima *et al.*; Tanggis, Characterization of the quasi-enveloped hepatitis e virus particles released by the cellular exosomal pathway. *J. Virol.* **91**, e00822-17 (2017).
42. S. Nagashima *et al.*, Hepatitis E virus egress depends on the exosomal pathway, with secretory exosomes derived from multivesicular bodies. *J. Gen. Virol.* **95**, 2166–2175 (2014).
43. C. C. Chen *et al.*, Elucidation of exosome migration across the blood-brain barrier model in vitro. *Cell. Mol. Bioeng.* **9**, 509–529 (2016).
44. L. Alvarez-Erviti *et al.*, Delivery of siRNA to the mouse brain by systemic injection of targeted exosomes. *Nat. Biotechnol.* **29**, 341–345 (2011).
45. D. Cao *et al.*, Pig model mimicking chronic hepatitis E virus infection in immunocompromised patients to assess immune correlates during chronicity. *Proc. Natl. Acad. Sci. U.S.A.* **114**, 6914–6923 (2017).
46. K. D. Rochfort, P. M. Cummins, The blood-brain barrier endothelium: A target for pro-inflammatory cytokines. *Biochem. Soc. Trans.* **43**, 702–706 (2015).
47. G. D. Salam *et al.*, Serum tumor necrosis factor-alpha level in hepatitis E virus-related acute viral hepatitis and fulminant hepatic failure in pregnant women. *Hepatol. Res.* **43**, 826–835 (2013).
48. N. Kamar, O. Marion, F. Abravanel, J. Izopet, H. R. Dalton, Extrahepatic manifestations of hepatitis E virus. *Liver Int.* **36**, 467–472 (2016).
49. A. Sood, V. Midha, N. Sood, Guillain-Barré syndrome with acute hepatitis E. *Am. J. Gastroenterol.* **95**, 3667–3668 (2000).
50. D. Todt *et al.*, Robust hepatitis E virus infection and transcriptional response in human hepatocytes. *Proc. Natl. Acad. Sci. U.S.A.* **117**, 1731–1741 (2020).
51. W. Yu *et al.*, Inhibition of hepatitis E virus replication by zinc-finger antiviral Protein synergizes with IFN-β. *J. Viral Hepat.* **28**, 1219–1229 (2021).
52. L. E. Gralinski, S. L. Ashley, S. D. Dixon, K. R. Spindler, Mouse adenovirus type 1-induced breakdown of the blood-brain barrier. *J. Virol.* **83**, 9398–9410 (2009).
53. C. Casiraghi, K. Dorovini-Zis, M. S. Horwitz, Epstein-Barr virus infection of human brain microvessel endothelial cells: A novel role in multiple sclerosis. *J. Neuroimmunol.* **230**, 173–177 (2011).
54. O. O. Koyuncu, I. B. Hogue, L. W. Enquist, Virus infections in the nervous system. *Cell Host Microbe* **13**, 379–393 (2013).
55. S. Dittmar *et al.*, Measles virus-induced block of transendothelial migration of T lymphocytes and infection-mediated virus spread across endothelial cell barriers. *J. Virol.* **82**, 11273–11282 (2008).
56. J. J. Miner, M. S. Diamond, Mechanisms of restriction of viral neuroinvasion at the blood-brain barrier. *Curr. Opin. Immunol.* **38**, 18–23 (2016).
57. B. Février, G. Raposo, Exosomes: Endosomal-derived vesicles shipping extracellular messages. *Curr. Opin. Cell Biol.* **16**, 415–421 (2004).
58. M. J. Haney *et al.*, Exosomes as drug delivery vehicles for Parkinson's disease therapy. *J. Control. Release* **207**, 18–30 (2015).
59. D. Ha, N. Yang, V. Nadithe, Exosomes as therapeutic drug carriers and delivery vehicles across biological membranes: Current perspectives and future challenges. *Acta Pharm. Sin. B* **6**, 287–296 (2016).
60. R. S. Klein *et al.*, Neuroinflammation during RNA viral infections. *Annu. Rev. Immunol.* **37**, 73–95 (2019).
61. D. J. DiSabato, N. Quan, J. P. Godbout, Neuroinflammation: The devil is in the details. *J. Neurochem.* **139** (suppl. 2), 136–153 (2016).
62. F. Piancone, F. La Rosa, I. Marventano, M. Saresella, M. Clerici, The role of the inflammasome in neurodegenerative diseases. *Molecules* **26**, 953 (2021).
63. S. Sil *et al.*, Role of inflammasomes in HIV-1 and drug abuse mediated neuroinflammaging. *Cells* **9**, 1857 (2020).
64. A. Sepehrinezhad, A. Gorji, S. Sahab Negah, SARS-CoV-2 may trigger inflammasome and pyroptosis in the central nervous system: A mechanistic view of neurotropism. *Inflammopharmacology* **29**, 1049–1059 (2021).
65. B. Weksler, I. A. Romero, P. O. Couraud, The hCMEC/D3 cell line as a model of the human blood brain barrier. *Fluids Barriers CNS* **10**, 16 (2013).
66. P. Shukla *et al.*, Adaptation of a genotype 3 hepatitis E virus to efficient growth in cell culture depends on an inserted human gene segment acquired by recombination. *J. Virol.* **86**, 5697–5707 (2012).
67. X. J. Meng *et al.*, Genetic and experimental evidence for cross-species infection by swine hepatitis E virus. *J. Virol.* **72**, 9714–9721 (1998).
68. S. Verma *et al.*, West Nile virus infection modulates human brain microvascular endothelial cells tight junction proteins and cell adhesion molecules: Transmigration across the in vitro blood-brain barrier. *Virology* **385**, 425–433 (2009).
69. N. Jothikumar, T. L. Cromeans, B. H. Robertson, X. J. Meng, V. R. Hill, A broadly reactive one-step real-time RT-PCR assay for rapid and sensitive detection of hepatitis E virus. *J. Virol. Methods* **131**, 65–71 (2006).
70. D. Tian *et al.*, Dissecting the potential role of hepatitis E virus ORF1 nonstructural gene in cross-species infection by using intergenotypic chimeric viruses. *J. Med. Virol.* **92**, 3563–3571 (2020).